International Journal of
Georesources and Environment
http://ijge.camdemia.ca, ijge@camdemia.ca
IJGE 2018 **4**(**2**): 33-39
Available at http://ojs.library.dal.ca/ijge

Materials Processing and Utilization

Atmospheric Corrosion Behavior of Mild Steel in the Initial Stage under Different Relative Humidity

Cui Lin[1,2*] and Sanjuan Chen[1]
[1] School of Materials Science and Engineering, Nanchang Hangkong University, Nanchang China 330063
[2] Mineral Resource Engineering, Dalhousie University, Halifax, Canada

Abstract: The corrosion behaviour of mild steel in the initial stage was studied in simulated pollutant-free atmosphere with relative humidity (RH) of 65%, 75% and 95%. The mass gain has a positive linear relationship with the exposure time. It increases significantly with the increase of relative humidity. The initiation and propagation of corrosion in the initial stage have a feature of filiform corrosion. An aeration cell is formed in a water droplet. Fe is dissolved to form Fe^{2+} in the center of the cell, and O_2 is reduced to produce OH^- at the edge of droplet. They move toward each other and react to form $Fe(OH)_2$. At this site, corrosion continues to generate cellular corrosion products. Some Fe^{2+} species flow forward to form a new active site as an anode. The old site acts as a cathode. The small anode-big cathode promotes the development of filaments. In case of high relative humidity, the corrosion is accelerated. The width of filaments and the growth rate of cellular corrosion products increase. Under RH65%, the dominant corrosion products are α-FeOOH and γ-FeOOH; while under RH75% and 95%, the corrosion products are mainly composed of γ-FeOOH, α-FeOOH, γ-Fe_2O_3 and Fe_3O_4.

Keywords: mild steel, relative humidity, atmospheric corrosion, mass gain, corrosion characteristics, initial stage

1 Introduction

Atmospheric corrosion is the result of interaction of a material with its surrounding atmospheric environment. It is the most common form of corrosion failure of metals in the natural environment.

There are two types of atmospheric corrosion according to the corrosion reaction: chemical and electrochemical corrosion (Wang et al 1997a). Tarnishing or discolor on a metal surface due to oxidation or sulfuration in dry atmosphere in the absence of significant water vapor is chemical corrosion. In this case, the corrosion rate is very low. In atmosphere with relative humidity of less than 100%, damp corrosion occurs under an invisible moisture film. When the metal surface is covered with a visible moisture film, wet corrosion forms. Damp and wet corrosion involve an electrochemical process. Accordingly, atmospheric corrosion is usually the electrochemical reaction which takes place under a thin moisture film. Under humid condition, the thickness and continuity of the electrolyte film as well as chemical composition in the electrolyte film are vital factors affecting the corrosion of metals in an atmosphere. The former is mainly caused by the atmospheric meteorological environment, and the latter is largely related to the air pollutants, such as SO_2, CO_2, H_2S, NO_x, and NaCl (Lin and Li 2004, Ahmad 2006, Lin and Li 2006).

Carbon steels are the most used metallic constructional materials because of their low price, high strength, welding and forming abilities. The applications of carbon steel in the atmosphere include buildings, bridges, pylons, cars, etc. However, carbon steels are susceptible to corrosion (Singh et al 2008, Lin et al 2018). They are easy to react with oxygen and moisture in the atmosphere. Rusting and failure as a result of atmospheric corrosion may cause accidents, for example, collapse of construction support and bridge.

In 1976 ASTM began the study of atmospheric corrosion of steel. National environmental corrosion testing stations were established in China in 1983 to start the corrosion data accumulation and corrosion behavior investigation for carbon steel exposed in atmospheric environment (Wang et al 1997b, Cao 2005, Lin et al 2005, Han et al 2007, Xiao and Li 2008). Long-term corrosion performances in rural, urban, industrial and marine atmospheres through field testing have been explored. The predominant corrosion products of carbon steel consist of iron oxyhydroxide (i.e. α-FeOOH, β-FeOOH, γ-FeOOH) and iron oxide (i.e. γ-Fe_2O_3, α-Fe_2O_3, Fe_3O_4). The type and content of corrosion products are closely relevant to the specific atmospheric environment (Hou 1999, Sei et al 1999, Santana Rodr guez 2002, Dong et al 2007, Ramesh and Singh 2009). For instance, the content of lepidocrocite (γ-FeOOH) in rural atmosphere is higher than that in industrial or marine atmosphere. γ-FeOOH is the relatively stable corrosion product which firstly appears. On the basis of the type of atmosphere, other different corrosion products grow. Regression analysis for the corrosion rate data in the long-

* Corresponding Author: Cui Lin, Email: cui.lin@dal.ca

DOI: 10.15273/ijge.2018.02.006

term exposure conditions indicates that it follows the power function. Since field studies normally require exposure times of several years, atmospheric corrosion is often studied by accelerated testing in the laboratory. It can be used to discuss the effects of one or a few typical environmental factors on the corrosion of metals (Nishikata et al 1997, Lin et al 2004a, Katayama 2005). The research of atmospheric corrosion of carbon steel in accelerated laboratory testing focuses on the corrosion mechanism in atmosphere containing pollutants (Lin et al 2004b). Different pollutants produce different effects on the corrosion characteristics, especially in the initial stage. In atmosphere with single SO_2, CO_2 and/or NaCl, the corrosion rate is accelerated compared with pollutant-free atmosphere (Pacheco et al 1990, Li et al 2009, Lin et al 2011, Lin and Xiao 2014). In SO_2-polluted atmosphere, corrosion of carbon steel has filiform characteristics. The growth of filament is associated with microstructure of carbon steel and is driven by the corrosion cells having anodes and cathodes in the small local area (Weissenrieder and Leygraf 2004, Lin et al 2010). In the presence of NaCl, CO_2 is inhibitive to corrosion of carbon steel owing to the growth of slightly soluble corrosion products (Lin and Li 2005); whereas SO_2 can promote corrosion for soluble corrosion products. The research found that relative humidity (RH) is the primary driving force for the occurrence of atmospheric corrosion. However, the role of RH in the atmospheric corrosion of carbon steel is not yet fully understood. The initiation and propagation of corrosion in atmosphere with different RH need to be further discussed.

The aim of this paper is to investigate the corrosion behavior of mild steel in pollutant-free atmosphere with different RH via measurement of corrosion rate, observation of morphology and analysis of evolution of corrosion products.

2 Experimental Method

2.1 Sample preparation

The test material used was mild steel with a size of Φ15 mm × 10 mm. It had a chemical composition of C 0.17, Si 0.17, Mn 0.35, P 0.035, Cr 0.25, Ni 0.30, S 0.035 and balance Fe (Mass percent, %). Before exposure to the simulated atmosphere, the samples were ground to 2000 grit with SiC grinding paper, and polished with a 2.5 μm diamond suspension. Then they were cleaned in absolute ethyl alcohol, dried in air, and stored in a desiccator for 24 h before testing.

2.2 Laboratory simulation test

A temperature and humidity testing chamber, which can regulate relative humidity from 30% to 98% and temperature from -20 °C to 150 °C was applied to perform the simulation test. As the experiments were carried out in the laboratory, the temperature was kept constant at 25 °C with an accuracy of ±2 °C. The relative humidity was controlled at 65%, 75%, and 95%, respectively. The duration for each experiment was 506 h.

2.3 Characterization methods

The mass of the sample was measured before and after exposure to obtain the mass gain using a Sartorius CP225D balance with a precision of 0.01 mg.

The microscopic changes on the surface was recorded by XJP-6A optical microscopy. The surface corrosion morphologies were observed by QUANTA200 scanning electron microscopy (SEM). At the same time, the element composition in the corrosion products was examined by an energy dispersive X-ray detector coupled to SEM.

Phases identification were performed by D_{MAX}-RB X-ray diffraction (XRD) operated at 40 kV and 150 mA using Cu K_α radiation. The diffraction patterns were collected from 10° to 100° 2θ at a step size of 0.02° 2θ. The valence state of the elements in the corrosion products was analyzed through X-ray photoelectron spectroscopy (XPS) manufactured by Rigaku Denki Co. Ltd working with an Al-K_α radiation source under 15 kV and 15 mA. The measurement was done at 2.3×10^{-8} MPa vacuum level.

3 Results and Discussion

3.1 Corrosion rate

The variation of mass gain with exposure time under the condition of different relative humidity is shown in Fig. 1. The mass gain increased with the increasing relative humidity. In all cases, the mass gain had a linear relationship with the exposure time, which can be expressed as Eq. (1).

$$\Delta m = kt + C \quad (1)$$

where Δm is the mass gain per unit area; t is the exposure time; C is related to the surface condition of carbon steel and k is a constant representing the corrosion rate. C and k values calculated using Eq. (1) are listed in Table 1. The magnitude of k varied in the sequence of $k_{95\%} > k_{75\%} > k_{65\%}$. This implies that the corrosion rate is significantly influenced by the moisture condition. With the increase of relative humidity, the moisture film on the surface of mild steel is thickened, that provides sufficient electrolyte for the corrosion reaction. This causes the acceleration of corrosion process.

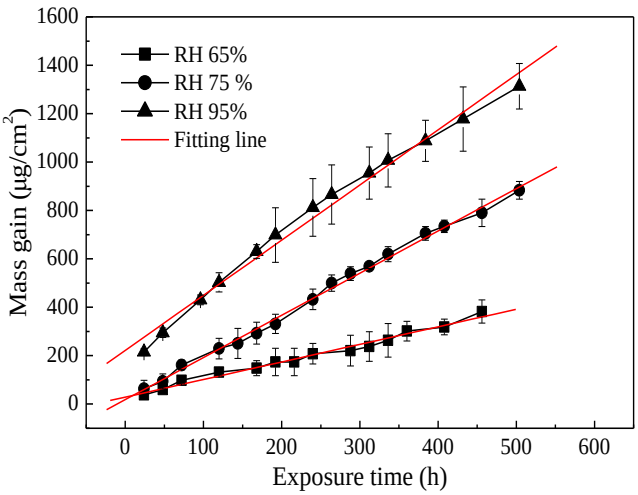

Fig. 1 Mass gain of mild steel as a function of time under the condition of different relative humidity

Table 1 *C* and *k* values calculated by using Eq. (1)

Relative humidity	*C*	*k*
65%	28.728	0.726
75%	18.287	1.743
95%	221.793	2.278

3.2 Corrosion morphology

3.2.1 OP images

The microscopic images on the surface of mild steel under different conditions are demonstrated in Fig. 2. Filiform corrosion occurred on the surface of mild steel. The filaments grew on the surface. They connected each other and form a network of ridges after 168 h. There were some cellular corrosion products which formed in local areas on the filaments. As the relative humidity increased, the filaments became wider.

3.2.2 SEM images

The morphologies on the surface of mild steel under the conditions of RH65%, 75% and 95% after different exposure time are shown in Figs. 3, 4 and 5, respectively.

In the case of RH65%, a number of thin filaments and a small amount of cellular corrosion products appeared on the surface after 168 h. With the continuation of test, filaments spread, and cellular corrosion products increased. Fig. 3d and e are a lower and higher magnification image for Fig. 3c, respectively. A lot of micro-cracks formed on the filiform and cellular corrosion products, and the cellular corrosion products grew in clusters.

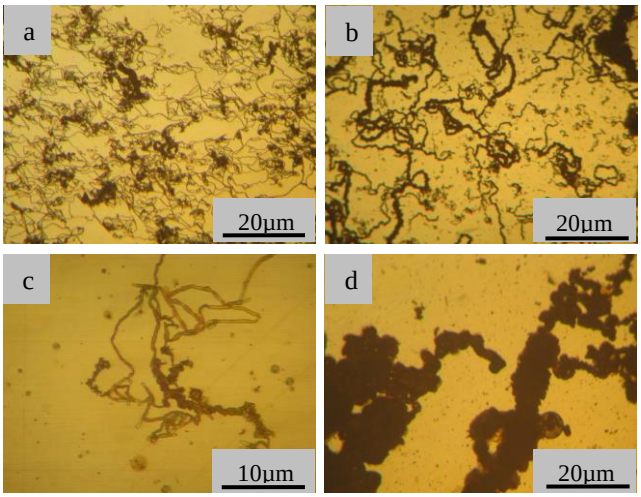

Fig. 2 OP images on the surface of mild steel under different conditions: (a) RH65%, 168 h; (b) RH75%, 168 h; (c) RH95%,168 h; (d) RH95%, 504 h

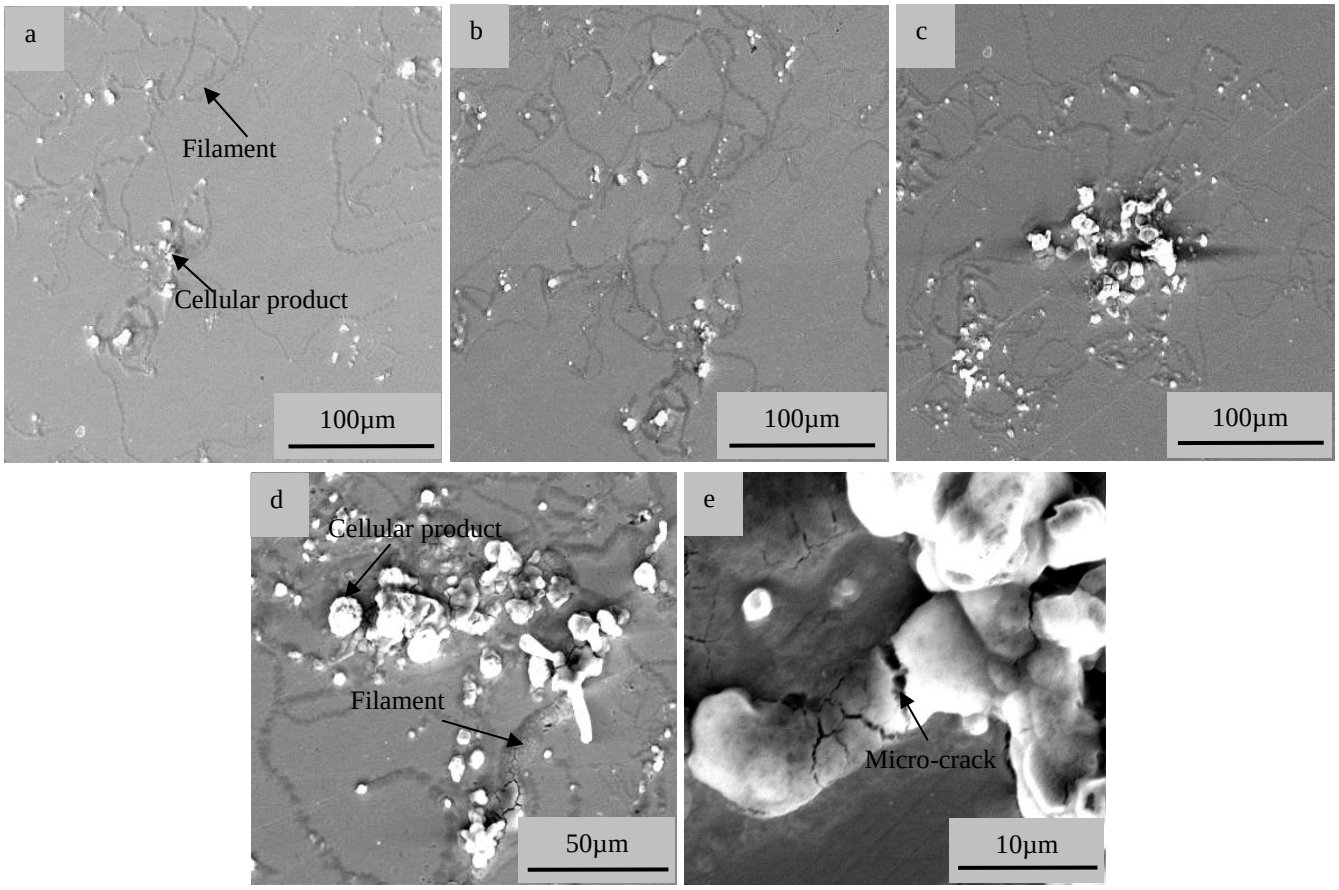

Fig. 3 SEM images of mild steel under the condition of RH65% for different time: (a) 168 h; (b) 336 h; (c) 504 h; (d) 504 h, magnification image; (e) 504 h, magnification image

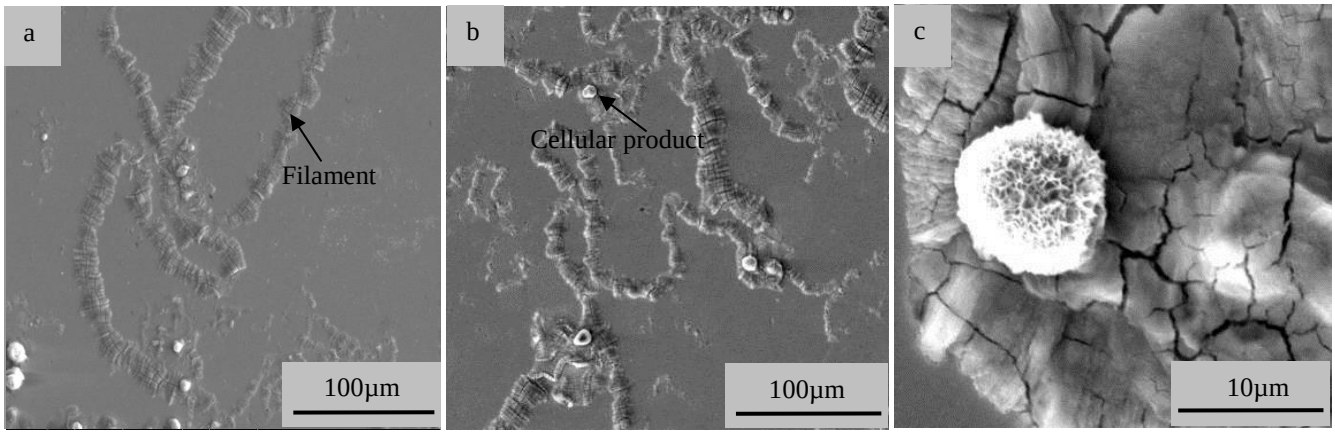

Fig. 4 SEM images of mild steel under the condition of RH75% for different time: (a) 144 h; (b) 312 h; (c) magnification image of cellular products labelled in (b)

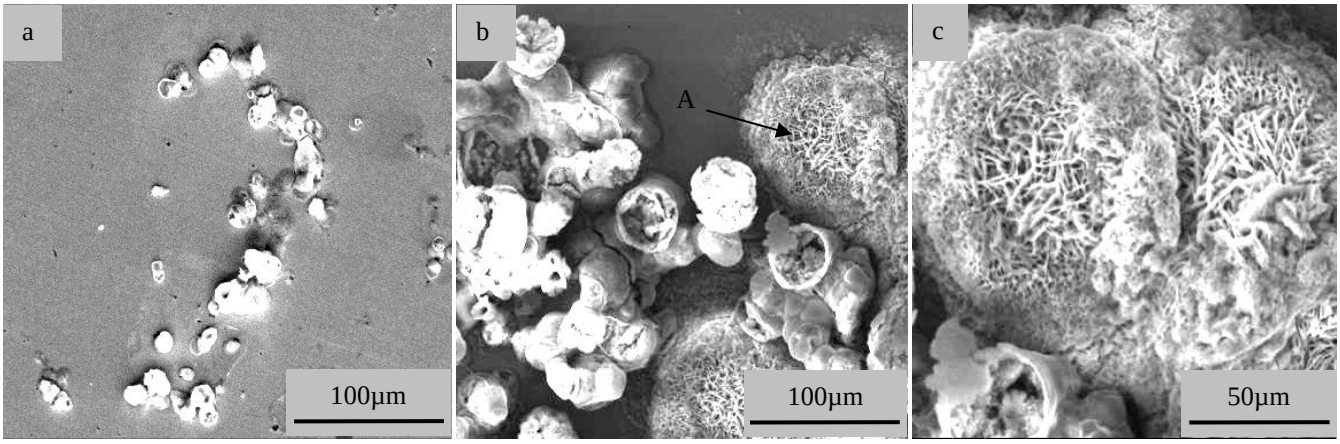

Fig. 5 SEM images of mild steel under the condition of RH95% for different time: (a) 144 h; (b) 336 h; (c) 336 h, magnification image for position A labelled in (b)

When RH was changed to 75%, in comparison with the case of RH65%, the wider filaments and obvious cracks can be observed. In the magnification image for cellular corrosion products, acicular corrosion products grew inside the cellular corrosion products.

When RH was increased to 95%, there were less and wider filaments on the surface, and more cellular corrosion products formed on the filaments. After 336 h, larger clusters of acicular corrosion products developed. This kind of corrosion product was found to be lepidocrocite (γ-FeOOH) or goethite (α-FeOOH) (Lin et al 2010). The top crust of some cellular corrosion products was open to the atmosphere, which enabled oxygen and water to easily penetrate into the substrate.

3.3 Composition of corrosion products

3.3.1 EDS

The EDS analysis results of elemental composition of corrosion products are given in Table 2. It can be seen from Table 2 that Fe and O existed in the corrosion products. The oxygen content in the cellular and acicular corrosion products was higher than that in the filaments.

Table 2 Content of the elements of corrosion products

RH	Elements	Filament	Cellular product	Acicular product
65%	Fe	59.47	31.82	—
	O	40.53	68.18	—
75%	Fe	69.62	38.54	—
	O	30.38	61.46	—
95%	Fe	66.36	38.24	32.37
	O	33.64	61.76	67.63

3.3.2 XRD

The XRD spectra of corrosion products of mild steel corroded under different humidity for 456 h are depicted in Fig. 6. The dominant corrosion products were α-FeOOH and γ-FeOOH in atmosphere with RH65%. In atmosphere with RH75% and 95%, the corrosion products were composed of γ-FeOOH, α-FeOOH, γ-Fe_2O_3 and Fe_3O_4.

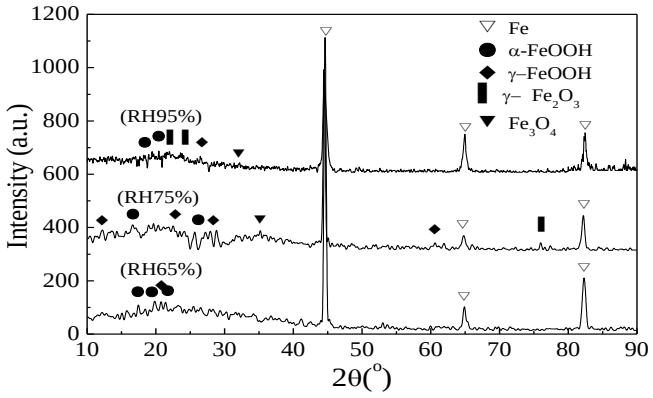

Fig. 6 XRD patterns of corrosion products of mild steel under different relative humidity for 456 h

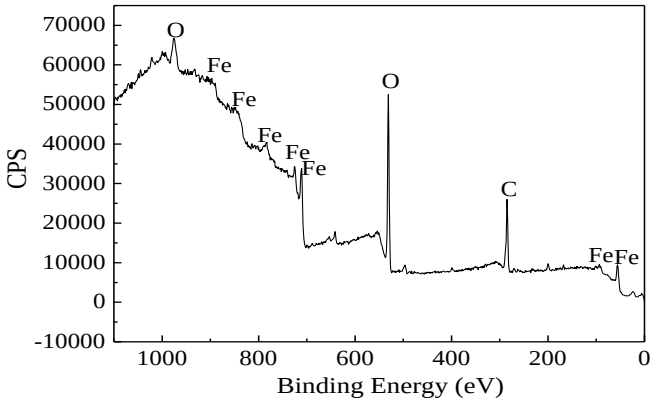

Fig. 7 XPS spectrum of corrosion products of mild steel under the condition of RH95% for 456 h

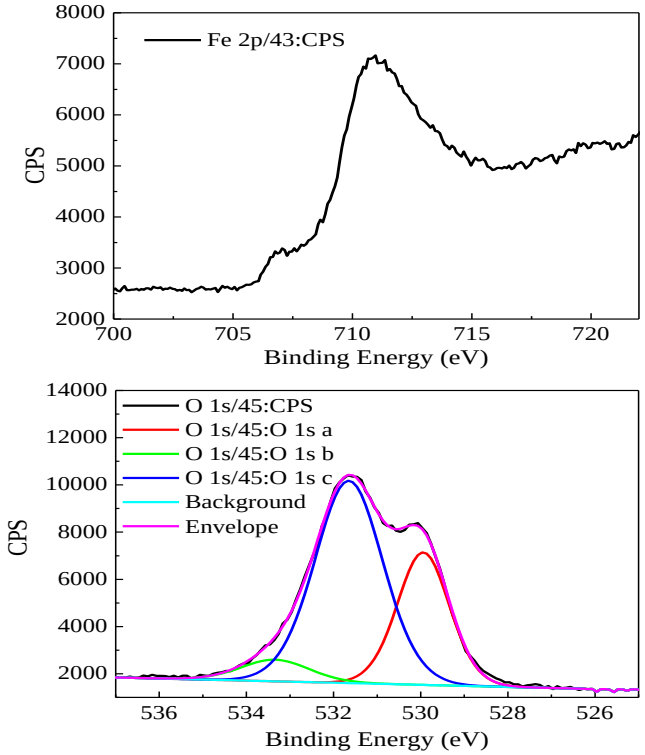

Fig. 8 XPS spectra of Fe and O in the corrosion products of mild steel under the condition of RH95% for 456 h

3.3.3 XPS

The XPS spectrum of corrosion products of mild steel corroded under RH 95% for 456 h is shown in Fig. 7. The analysis results also indicate that the elements dominated in the corrosion products on the surface were oxygen and iron.

To evaluate the chemical state of Fe and O in the corrosion products, the XPS spectra for Fe_{2p} and O_{1s} were further analyzed (Fig. 8). Table 3 gives the binding energy in the peaks in the spectra and reference values for species containing Fe and O. The peaks in the spectrum of Fe appeared at the binding energy of 711.51eV, 708.76eV and 706.7eV. These correspond to the binding energy for Fe2p3/2 (711.8eV) of Fe^{3+}, Fe2p3/2 (708.3.5eV) of $Fe(OH)_2$ and 706.5eV of iron (Lin et al 2012).

Table 3 Binding energy in the peaks in the spectra and reference values for species containing Fe and O

Species	Binding energy in the peaks in the spectra (eV)	Reference Binding energy (eV)	Area (%)
O^{2-}	529.9	529.94	31.23
OH^-	531.4	531.65	62.14
H_2O	533.2	533.34	6.67
Fe^{3+}	711.51	711.8	94.84
$Fe(OH)_2$	708. 76	708.35	3.45
Fe	706.7	706.5	0.72

The XPS spectrum of O can be divided into three peak curves, revealing that O has three chemical states in the corrosion products. According to the reference binding energy, the first is M-O compound peak, which corresponds to O^{2-}. This indicates that there may be Fe_3O_4 and Fe_2O_3 existing in the corrosion products; the second is characteristic peak of compound M-OH or M-$(OH)_2$, which corresponds to OH^-. This reveals the existence of FeOOH. From the peak area, the corrosion products mainly consisted of FeOOH; the third is characteristic peak of H_2O. Integrated with the analysis result of Fe, it can be inferred that the main corrosion products contained FeOOH, and a little $Fe(OH)_2$, Fe_3O_4 and Fe_2O_3.

4 Corrosion Mechanism Analysis

The relative humidity in atmosphere affects the evolution of corrosion process on the surface of mild steel.

Atmospheric corrosion process in the initial stage of mild steel includes the following steps in pollutant-free air:

(1) Water molecular absorbs on the surface and water droplets form;

(2) The electrochemical corrosion process starts in the water droplet. Ferric dissolution occurs in the anodic region, the cathodic reaction is oxygen reduction.

Anodic reaction:

$$Fe \rightarrow Fe^{2+} + 2e^- \qquad \text{(reaction 1)}$$

Cathodic reaction:

$$O_2+2H_2O+4e^-\rightarrow 4OH^- \quad \text{(reaction 2)}$$

Oxygen reduction results in the formation of hydroxide ions, causing an increase in pH at the cathodic site.

(3) Fe^{2+} reacts with OH^- to form ferrous hydroxide.

$$Fe^{2+} + H_2O\rightarrow Fe(OH)^+ + H^+ \quad \text{(reaction 3)}$$

$$Fe(OH)^+ + H_2O\rightarrow Fe(OH)_2+H^+ \quad \text{(reaction 4)}$$

(4) $Fe(OH)_2$ is unstable in the presence of oxygen. It reacts with oxygen to form γ-FeOOH. With the decrease of pH in the electrolyte film, and γ-FeOOH is converted into α-FeOOH.

$$2Fe(OH)_2+1/2\ O_2\rightarrow 2FeOOH+ H_2O \quad \text{(reaction 5)}$$

(5) Some of FeOOH is decomposed to produce Fe_2O_3. Fe_2O_3 is further oxidized to generate Fe_3O_4.

$$2FeOOH \rightarrow Fe_2O_3 + H_2O \quad \text{(reaction 6)}$$

$$Fe_2O_3 + O_2\rightarrow Fe_3O_4 \quad \text{(reaction 7)}$$

At the beginning, an aeration cell is formed in the droplet, where iron starts to dissolve and Fe^{2+} moves towards the cathodic area (Fig. 9a). When Fe^{2+} meets with OH^-, $Fe(OH)_2$ is formed. $Fe(OH)_2$ reacts with oxygen and water to generate γ-FeOOH and α-FeOOH, which are cellular and acicular corrosion products shown in OP and SEM images. Some Fe^{2+} species are still in an active state and flow forward to form a new active site as an anode, and the formed cellular corrosion products serve as a big cathode, constituting a new corrosion cell (Fig. 9b). This promotes the growth of filaments (Fig. 9c).

With the increase of relative humidity, bigger water droplets form, under the condition of RH95%, the continuous and thick electrolyte film formed on the surface quickly. This leads to the increase of oxygen absorption and then accelerates the reaction rate in each step. Hence, the width of filaments and the amount of cellular corrosion products are increased.

5 Conclusions

(1) In pollutant-free atmosphere, the mass gain follows linear growth law during the corrosion period of 504 h. The mass gain increases with the increasing relative humidity.

(2) The corrosion of mild steel has filiform corrosion characteristics, meanwhile cellular corrosion products grow on the filaments. In case of RH65%, the dominant corrosion products are α-FeOOH and γ-FeOOH. Under the conditions of RH75% and 95%, the corrosion products are mainly composed of γ-FeOOH, α-FeOOH, γ-Fe_2O_3 and Fe_3O_4.

(3) The evolution of corrosion process in the initial stage has a filiform corrosion characteristic. Meanwhile cellular products form on the filaments. With the increase in relative humidity, the corrosion is accelerated. Consequently, the filaments become wider and cellular corrosion products grow faster.

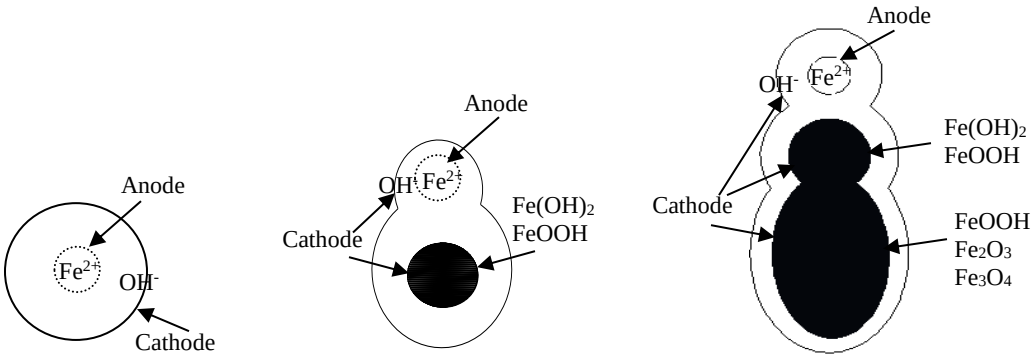

Fig. 9 Schematic diagram of formation of filiform corrosion products in the environment: (a) formation of an aeration cell; (b) formation of a new cell; (c) the growth of filament

Acknowledgement

This study was supported by National Natural Science Foundation of China (No. 50601012).

References

Ahmad, Z., 2006. Principles of Corrosion Engineering and Corrosion Control. Elsevier, Great Britain, pp550 - 554.

Cao, C.N., 2005. Corrosion in Natural Environment of Materials in China. Chemical Industry Press, Beijing, pp2 - 6, 69 - 73. (in Chinese)

Dong, J.H., E.H. Han and K. Wei, 2007. Introduction to atmospheric corrosion research in China. Science and Technology of Advanced Materials, **8**: 559 - 565.

Han, W., G.C. Yu, Z.Y. Wang and J. Wang, 2007. Characterisation of initial atmospheric corrosion carbon steels by field exposure and laboratory simulation. Corrosion Science, **49**(**7**): 2920 - 2935.

Hou, W. and C. Liang, 1999. Eight-year atmospheric corrosion exposure of steels in China. Corrosion, **55**(**1**): 65 - 73.

Katayama, H, K. Noda, H. Masuda, M. Nagasawa, M. Itagaki and K. Watanabe, 2005. Corrosion simulation of carbon steels in atmospheric environment. Corrosion Science, **47**: 2599 - 2606.

Li, X.G., C.F. Dong, K. Xiao, C.W. Du and H.R. Zhou, 2009. Initial Atmospheric Corrosion Behavior and Mechanism

of Metals. Science Press, Beijing. (in Chinese)

Lin, C. and X.G. Li, 2004. Initial stages of corrosion behaviors for AZ91 magnesium alloy in the presence of SO_2. Journal of University of Science and Technology Beijing: Mineral Metallurgy Materials, **11**(**5**): 433 - 441.

Lin, C., F.P. Wang and X.G. Li, 2004a. The progress of research methods on atmospheric corrosion. Journal of Chinese Society for Corrosion and Protection, **24**(**4**): 249 - 256. (in Chinese)

Lin, C., X.G. Li and G.Y. Wang, 2004b. Research progress on initial stage of atmospheric corrosion behavior of metals in pollutant atmospheres. Corrosion Science and Protection Technology, **16**(**2**): 89 - 95. (in Chinese)

Lin, C. and X.G. Li, 2005. Initial CO_2-induced Atmospheric Corrosion of Carbon Steel in the Presence of NaCl. 16th International Corrosion Conference, Beijing, China. September 19 - 24, 2005.

Lin, C., X.G. Li and X.D. Li, 2005. The initial stage of atmospheric corrosion of carbon and weathering steel in Beijing city atmosphere. Journal of Chinese Society for Corrosion and Protection, **25**(**4**): 193 - 199. (in Chinese)

Lin, C. and X.G. Li, 2006. Role of CO_2 in the initial stage of atmospheric corrosion of AZ91 magnesium alloy in the presence of NaCl. Rare Metals, **25**(**2**): 190 - 196.

Lin, C., Q. Zhao and Y.E. Liu, 2010. Evolution of corrosion products of 20 carbon steel in atmosphere containing SO_2. Acta Metallurgica Sinica, **46**(**3**): 358 - 365. (in Chinese)

Lin, C., S.J. Chen, W. He and L.C. Zhao, 2011. Effect of acid rain on corrosion behavior of mild steel. Journal of Iron and Steel Research, **23**(**6**): 18 - 23. (in Chinese)

Lin, C., S.J. Chen and Z.Y. Xiao, 2012. Effect of humidity on corrosion behavior of low carbon steel in atmosphere containing SO_2. Materials for Mechanical Engineering, **36**(**1**): 16 - 22. (in Chinese)

Lin, C. and Z.Y. Xiao, 2014. Electrochemical corrosion behavior of carbon steel under thin electrolyte layer containing NaCl. Corrosion & Protection, **35**(**4**): 316 - 320. (in Chinese)

Lin, C., Q. Zhao, X.B. Zhao and Y. Yang, 2018. Cavitation Erosion of Metallic Materials. International Journal of Georesources and Environment, **4**(**1**): 1 - 8.

Nishikata, A., Y. Ichihara, Y. Hayashi and T. Tsuru, 1997. Influence of electrolyte layer thickness and pH on the initial stage of the atmospheric corrosion of iron. Journal of Electrochemical Society, **144**(**4**): 1244 - 1252.

Pacheco, A.M.G., M.G.I.B. Teixeira and M.G.S. Ferreira, 1990. Initial stages of chloride induced atmospheric corrosion of iron: an infrared spectroscopic study. British Corrosion Journal, **25**(**1**): 57 - 59.

Ramesh, A.V. and K.N. Singh, 2009. Conversion electron Mössbauer spectroscopy study of growth and nature of corrosion products on mild steel exposed to different environments. Hyperfine Interactions, **188**(**1-3**): 51 - 58.

Santana Rodríguez, J.J., F.J. Santana Hernandez, J.E. González González, 2002. Mathematical and electro-chemical characterisation of the layer of corrosion products on carbon steel in various environments. Corrosion Science, **44**(**11**): 2597 - 2610.

Sei, J.O., D.C. Cook and H.E. Townsend, 1999. Atmospheric corrosion of different steels in marine, rural and industrial enviroments. Corrosion Science, **41**(**9**): 1687 - 1702.

Singh, D.D.N., S. Yadav and J.K. Saha, 2008. Role of climatic conditions on corrosion characteristics of structural steels. Corrosion Science, **50**(**1**): 93 - 110.

Wang, G.Y., H.J. Wang and X.L. Li, 1997a. Corrosion and Protection in Natural Environment-Atmosphere, Marine, Soil. Chemical Industry Press, Beijing, pp5 - 10. (in Chinese)

Wang, J.H., F.I. Wei, Y.S. Chang and H.C. Shih, 1997b. The corrosion mechanisms of carbon steel and weathering steel in SO_2 polluted atmospheres. Materials Chemistry and Physics, **47**: 1 - 8.

Weissenrieder, J. and C. Leygraf, 2004. In situ studies of filiform corrosion of iron. Journal of the Electrochemical Society, **151**(**3**): B165 - B171.

Xiao, K. and X.G. Li, 2008. Corrosion products and formation mechanism during initial stage of a corrosion of carbon steel. Iron and Steel Research, **15**(**5**): 42 - 48.